Inorg. Chem. **2005**, *44*, 8786–8793

$Sn_{19.3}Cu_{4.7}As_{22}I_8$: a New Clathrate-I Compound with Transition-Metal Atoms in the Cationic Framework

Kirill A. Kovnir,[†,§,⊥] Alexei V. Sobolev,[‡] Igor A. Presniakov,[‡] Oleg I. Lebedev,[∥,#] Gustaaf Van Tendeloo,[∥] Walter Schnelle,[§] Yuri Grin,[§] and Andrei V. Shevelkov*[,†]

Inorganic Synthesis Laboratory and Chair of Radiochemistry, Moscow State University, 119992 Moscow, Russia, Max-Planck-Institut für Chemische Physik fester Stoffe, 01187 Dresden, Germany, and EMAT, University of Antwerp, B-2020 Antwerpen, Belgium

Received July 12, 2005

$Sn_{19.3}Cu_{4.7}As_{22}I_8$, a new clathrate-I compound with a cationic host framework containing transition metals, has been synthesized, and its crystal structure has been determined. It crystallizes in the cubic space group $Pm\bar{3}n$ with a unit cell parameter $a = 11.1736(3)$ Å and $Z = 1$ ($R = 0.031$ for 329 independent reflections and 22 variables). Tin, copper, and arsenic form the cationic clathrate framework hosting the guest iodine anions in cages of two different shapes. $Sn_{19.3}Cu_{4.7}As_{22}I_8$ does not contain vacancies in the framework but reveals three partially occupied positions of the metal atoms, leading to the formation of Sn–Sn and Sn–Cu bonds that differ in length. The ^{119}Sn Mössbauer spectrum confirms the local environment of tin atoms. The hyperfine constants obtained from the Mössbauer spectra for different cationic tin clathrates are discussed. Electron diffraction and electron microscopy reveal that the splitting affects the short-range ordering but does not lead to a superstructure. Though containing a transition metal, $Sn_{19.3}Cu_{4.7}As_{22}I_8$ is diamagnetic, and its composition corresponds to the Zintl formalism.

Introduction

A large family of inclusion compounds characterized by a complete sequestering of guest particles by a host framework is known as clathrates.[1] A first clathrate, the chlorine hydrate, was synthesized in 1811 by Davy.[2] Its crystal structure was determined 150 years later by Powell.[3] Afterward, a great number of hydrates of different molecules with seven types of clathrate structures were found.[4] The intermetallic compounds having the chlorine hydrate structure type, also known as the clathrate-I structure type, were discovered shortly after.[5,6] The majority of these compounds are narrow-gap semiconductors and, in general, Zintl phases.[7−9] Such clathrates are typically anionic because their frameworks are composed of group 13 and 14 metals acquiring electrons from group 1 and 2 metals or europium, which serve as guests; these compounds are briefly surveyed in a review.[10] Clathrates with the reversed host−guest polarity are also known.[11−18] In these compounds, the cationic

* To whom correspondence should be addressed. E-mail: shev@inorg.chem.msu.ru. Inorganic Synthesis Laboratory, Department of Chemistry, Moscow State University, Leninskie Gory 1/3, 119992 Moscow, Russia. Fax: (+7-095) 939 47 88.

† Inorganic Synthesis Laboratory, Moscow State University.

‡ Chair of Radiochemistry, Moscow State University.

§ Max-Planck-Institut für Chemische Physik fester Stoffe.

∥ University of Antwerp.

⊥ Present address: Department of Inorganic Chemistry, Fritz-Haber-Institut der MPG, 14195 Berlin, Germany.

On leave from the Institute of Crystallography RAS, 117333 Moscow, Russia.

(1) Wells, A. F. *Structural Inorganic Chemistry*, 5th ed.; Clarendon Press: Oxford, U.K., 1986; Chapter 15.
(2) Davy, H. *Philos. Trans. R. Soc. London* **1811**, *101*, 155.
(3) Powell, H. *J. Chem. Soc.* **1948**, *45*, 61−73.
(4) *Inclusion Compounds*; Atwood, J. L., Davies, J. E. D., MacNicol, P. D., Eds.; Academic Press: London, 1984.
(5) Cros, C.; Pouchard, M.; Hagenmuller, P. *C.R. Acad. Sci. Paris* **1965**, *260*, 4764−4797.
(6) Kasper, J. S.; Hagenmuller, P.; Pouchard, M. *Science* **1965**, *150*, 1713−1714.
(7) Miller, G. J. In *Chemistry, Structure, and Bonding of Zintl Phases and Ions*; Kauzlarich, S. M., Ed.; VCH: New York, 1996 and references cited therein.
(8) Paschen, S.; Carrillo-Cabrera, W.; Bentien, A.; Tran, V. H.; Baenitz, M.; Grin Yu.; Steglich, F. *Phys. Rev. B* **2001**, *64*, 214404 (1−11).
(9) Kovnir, K. A.; Shevelkov, A. V. *Russ. Chem. Rev.* **2004**, *73*, 923−938.
(10) Bobev, S.; Sevov, S. C. *J. Solid State Chem.* **2000**, *153*, 92−105.
(11) von Schnering, H. G.; Menke, H. *Angew. Chem.* **1972**, *84*, 30−31.
(12) Menke, H.; von Schnering, H. G. *Z. Anorg. Allg. Chem.* **1973**, *395*, 223−238.
(13) Nesper, R.; Curda, J.; von Schnering, H. G. *Angew. Chem., Int. Ed. Engl.* **1986**, *25*, 350−352.
(14) Shatruk, M. M.; Kovnir, K. A.; Shevelkov, A. V.; Presniakov, I. A.; Popovkin, B. A. *Inorg. Chem.* **1999**, *38*, 3455−3457.
(15) Shatruk, M. M.; Kovnir, K. A.; Shevelkov, A. V.; Popovkin, B. A. *Zh. Neorg. Khim.* **2000**, *45*, 203−209; *Russ. J. Inorg. Chem.* **2000**, *45*, 153−159.

10.1021/ic051160k CCC: $30.25
Published on Web 10/13/2005

framework is built up from pnictogen and group 14 metal atoms, and the halogen anions serve as guests. Various aspects of chemical studies of both anionic and cationic clathrates, their classification, the crystal and electronic structures, the properties, and the methods of synthesis of semiconducting clathrates are surveyed in a recent review.[9]

Clathrates with the type I structure based on the group 14 elements trigger growing interest because of the expectations that thermoelectric materials of a new generation will emerge following the guidelines of the "Phonon Glass, Electron Crystal" (PGEC) concept.[19,20] The correspondence of the clathrates to the PGEC concept was probed and questioned in a number of papers.[21−23] In light of their promising properties, the search for new clathrates, especially those containing heavy atoms and d metal atoms in the framework, and the gain of knowledge of the peculiarities of their crystal and electronic structure are of particular interest.

In this work, we report the synthesis and characterization of a new cationic clathrate $Sn_{19.3}Cu_{4.7}As_{22}I_8$ by means of X-ray diffraction, Mössbauer spectroscopy, and electron microscopy. We discuss the fine splitting of the positions and local ordering in the three-dimensional framework of the clathrate-I structure, which does not lead to any superstructure. The local electronic structure around the tin atoms in various cationic clathrates is analyzed on the basis of the Mössbauer data. Despite the presence of the transition metal, copper, $Sn_{19.3}Cu_{4.7}As_{22}I_8$ is a diamagnet and conforms to the Zintl electron-counting scheme for valence compounds.

Experimental Section

Starting Materials. Metallic tin, gray arsenic, and crystalline iodine (all from Reakhim, 99.99%) were used as received. Tin(IV) iodide was synthesized by the reaction of excess tin with iodine in CCl_4 according to the literature.[24] Copper powder (Reakhim, 99.9%) was preliminarily heated in a hydrogen flow at 775 K to remove traces of copper oxide.[25]

Synthesis. For the synthesis of $Sn_{19.3}Cu_{4.7}As_{22}I_8$, the stoichiometric mixture of tin, copper, gray arsenic, and tin(IV) iodide (total weight 1 g) was mixed and sealed in a silica tube under vacuum, and the load was heated at 723 K for 5 days. After cooling to room temperature, the sample appeared, according to the X-ray analysis (Huber G670 image plate camera, Cu Kα_1 radiation, $\lambda = 1.540\,598$ Å), as tiny black crystals of the desired clathrate phase contaminated with small amounts of tin(IV) iodide and SnAs and unidentified minor products. The sample was then reground, heated in a sealed silica ampule at 723 K for another 14 days, and then furnace-cooled. After the second annealing, the sample appeared as a black air- and moisture-stable homogeneous powder. X-ray analysis showed the presence of only one low-intensity peak ($I < 1\%$ of the strongest peak) of SnAs, with all other diffraction peaks belonging to the target clathrate phase. The diffraction pattern of $Sn_{19.3}Cu_{4.7}As_{22}I_8$ was indexed in the cubic system. The unit cell parameter $a = 11.1736(3)$ Å was obtained from the least-squares fit of the Guinier pattern using LaB_6 ($a = 4.156\,92$ Å) as an internal standard.[26] All attempts to synthesize $Sn_{24-x}Cu_xAs_{22}I_8$ compounds with $x > 4.7$ at 723 K were unsuccessful. The annealed products always appeared as multiphase mixtures of the cubic clathrate phase ($a \approx 11.173$ Å) with tin and copper arsenides and copper(I) iodide.

Table 1. Crystallographic Data for $Sn_{19.3}Cu_{4.7}As_{22}I_8$[a]

chemical formula	$Sn_{19.3(4)}Cu_{4.7(4)}As_{22}I_8$
formula weight	5236.25
space group	$Pm\bar{3}n$ (No. 223)
T [K]	290
cell parameter a [Å]	10.172(1)
V [Å^3]	1394.4(2)
Z	1
λ	0.710 69
density (calc) [g cm^{-3}]	6.236
μ [mm^{-1}]	27.586
R1,[b] wR2[c]	0.033, 0.063

[a] Further details of the crystal structure determination may be obtained from Fachinformationszentrum Karlsruhe, D-76344 Eggenstein-Leopoldshafen, Germany, upon quoting the depository number CSD-415578. [b] $R1 = \sum||F_o| - |F_c||/\sum|F_o|$. [c] $wR2 = [\sum w(F_o^2 - F_c^2)^2/\sum w(F_o^2)^2]^{1/2}$; $w = [\sigma^2(F_o^2) + Ap^2 + Bp]^{-1}$; $p = (F_o^2 + 2F_c^2)/3$; $A = 0.01$; $B = 3.4402$.

Single-Crystal X-ray Diffraction. A suitable single crystal of $Sn_{19.3}Cu_{4.7}As_{22}I_8$ selected from the product of the first annealing of the sample having a stoichiometric composition was glued with epoxy cement on the tip of a Pyrex fiber and mounted on a goniometer head of a CAD-4 (Nonius) diffractometer. The orientation matrix was refined on the basis of 24 well-centered reflections in the angular range of $28° < 2\theta < 30°$, and the derived lattice parameter ($a = 11.172(1)$ Å) agreed well with that found from the powder data for a bulk sample. X-ray data were recorded at room temperature and corrected for polarization and Lorentz effects. A semiempirical absorption correction was applied based on azimuthal scans of nine reflections having χ angles close to 90°. Further experimental parameters are listed in Table 1.

Crystal Structure Refinement. The crystal structure of $Sn_{19.3}Cu_{4.7}As_{22}I_8$ was solved in the space group $Pm\bar{3}n$ by direct methods (SHELXS-97)[27] that allowed the location of all atomic positions in the ideal clathrate-I structure. During the crystal structure refinement, the splitting of the 24-fold metal site was found. The final refinement (SHELXL-97)[28] converged at $R = 0.031$ for the composition $Sn_{19.3(4)}Cu_{4.7(4)}As_{22}I_8$. Further details are given under the Results and Discussion section. The atomic parameters are listed in Table 2, and selected interatomic distances and bond angles are presented in Table 3.

(16) Shatruk, M. M.; Kovnir, K. A.; Lindsjö, M.; Presniakov, I. A.; Kloo, L. A.; Shevelkov, A. V. *J. Solid State Chem.* **2001**, *161*, 233−242.
(17) Kovnir, K. A.; Zaikina, J. V.; Reshetova, L. N.; Olenev, A. V.; Dikarev, E. V.; Shevelkov, A. V. *Inorg. Chem.* **2004**, *43*, 3230−3236.
(18) Kovnir, K. A.; Uglov, A. N.; Zaikina, J. V.; Shevelkov, A. V. *Mendeleev Commun.* **2004**, *14*, 135−136.
(19) Slack, G. A. In *CRC Handbook of Thermoelectrics*; Rowe, D. M., Ed.; Chemical Rubber: Boca Raton, FL, 1995.
(20) Nolas, G. S.; Slack, G. A.; Schjuman, S. B. In *Recent Trends in Thermoelectric Materials Research*; Tritt, T. M., Ed.; Academic Press: San Diego, 2001.
(21) Paschen, S.; Pacheco, V.; Bentien, A.; Sanchez, A.; Carrillo-Cabrera, W.; Baenitz, M.; Iversen, B. B.; Grin, Yu.; Steglich, F. *Phys. B (Amsterdam, Neth.)* **2003**, *328*, 39−43.
(22) Bentien, A.; Christensen, M.; Bryan, J. D.; Sanchez, A.; Paschen, S.; Steglich, F.; Stucky, G. D.; Iversen, B. B. *Phys. Rev. B* **2004**, *69*, 045107 (1−5).
(23) Iversen, B. B.; Palmqvist, A. E. C.; Cox, D. E.; Nolas, G. S.; Stucky, G. D.; Blake, N. P.; Metiu, H. *J. Solid State Chem.*, **2000**, *149*, 455−458.
(24) *Handbuch der Präparativen Anorganischen Chemie*; Brauer, G., Ed.; Ferdinand Enke Verlag: Stuttgart, Germany, 1975.
(25) Karyakin, Yu. V.; Angelov, I. I. *Pure Chemicals*; Chemistry: Moscow, 1974.
(26) This value is very close to that found after the first annealing, $a = 11.174(1)$. The worse accuracy of the latter determination is attributed to the overlap of some peaks of the clathrate phase and admixtures.
(27) Sheldrik, G. M. *SHELXS-97, program for crystal structure solution*; University of Göttingen: Göttingen, Germany, 1997.
(28) Sheldrik, G. M. *SHELXL-97, program for crystal structure refinement*; University of Göttingen: Göttingen, Germany, 1997.

Table 2. Atomic Coordinates, Site Occupancy Factors (sof's), and Equivalent Displacement Parameters for $Sn_{19.3}Cu_{4.7}As_{22}I_8$

atom	site	*x*/*a*	*y*/*b*	*z*/*c*	sof	U_{eq}[a]
I(1)	2a	0	0	0	1	0.0091(4)
I(2)	6d	$^1/_2$	0	$^1/_4$	1	0.0182(4)
As(1)	6c	$^1/_4$	0	$^1/_2$	1	0.0196(5)
As(2)	16i	0.18766(5)	*x*	*x*	1	0.0136(3)
Sn(31)	24k	0.1261(6)	0	0.3098(3)	0.60(1)	0.0099(8)[b]
Sn(32)	24k	0.0850(9)	0	0.3261(5)	0.20(1)	0.020(1)[b]
Cu(33)	24k	0.1423(14)	0	0.2980(11)	0.20(3)	0.006(3)[b]

[a] U_{eq} is defined as one-third of the trace of the orthogonalized U_{ij} tensor. [b] Atoms were refined isotropically.

Chemical analysis was performed by inductively coupled plasma optical emission spectrometry methods using a Varian Vista RL spectrometer. A crop of crystals grown in the silica tube after the first annealing was mechanically picked for the analysis. For the sample preparation, an acid digestion method ($HCl:HNO_3 = 8:1$) was employed. All values are the average of at least three replicates.

Mössbauer Spectroscopy. The ^{119}Sn spectra were recorded using a conventional constant-acceleration Mössbauer spectrometer. Measurements were performed at 300 K, with the $Ca^{119m}SnO_3$ source maintained at room temperature. Isomer chemical shifts are referenced to a $CaSnO_3$ absorber at 300 K.

Transmission Electron Microscopy (TEM). Electron diffraction (ED) and high-resolution electron microscopy (HREM) investigations were performed using a JEOL 4000EX microscope operating at 400 kV. The sample for TEM was crushed, dispersed in methanol, and deposited on a holey carbon grid. Simulation of the HREM images was performed using Mac Tempas and Crystal Kit software.

Physical Measurements. The magnetic susceptibility χ was measured in fields of 3.5 and 7 T between 2 and 300 K using a SQUID magnetometer (Quantum Design).

Results and Discussion

$Sn_{19.3}Cu_{4.7}As_{22}I_8$ is a new compound belonging to the clathrate-I type. Its crystal structure is based on a three-dimensional framework comprised of Sn, Cu, and As atoms. The I atoms reside in the framework cavities with a 20-vertex dodecahedron occupied by the I(1) atom and a 24-vertex tetrakaidecahedron filled with the I(2) atom. In the regular type-I clathrate structure, the framework atoms occupy three positions, 24k, 16i, and 6c, of the space group $Pm\bar{3}n$ (Figure 1).[6] At the first step, the crystal structure of $Sn_{19.3}Cu_{4.7}As_{22}I_8$ was solved in the space group $Pm\bar{3}n$ by direct methods. The 16-fold and 6-fold positions were set as As, while the 24-fold site was set as Sn. The analysis of a difference Fourier density map after an isotropic refinement revealed two maxima lying close (ca. 0.5 Å) to the position of the Sn atom (Figure 2). All three positions were set as Sn of variable occupancy, with the sum of the occupancies being constrained at unity. The following refinement showed that the displacement parameter for one of the Sn positions was considerably higher than the parameters of the other two. This position was set as Cu. The refinement showed that the occupancies for the tin position Sn(32) and for the copper position Cu(33) are practically the same in the independent refinement but differ significantly from that for the Sn(31) atom. It was also found that the occupancy factors for all I and As atoms do not deviate from unity. The final refinement with the anisotropic displacement parameters for all but Sn and Cu atoms led to $R = 0.031$, giving the composition $Sn_{19.3(4)}Cu_{4.7(4)}As_{22}I_8$, which is in good agreement with the chemical analysis data. Found: 35.4(5):10.3(3):40.6(3):13.7-(2). Calculated for $Sn_{19.3(4)}Cu_{4.7(4)}As_{22}I_8$: 35.7(7):8.7(7):40.7:14.8. All attempts to describe the electron density near the 24k site as two instead of three neighboring metal positions with partial occupancies resulted in a notably higher *R* value and higher peaks in the difference Fourier map.

In the structure of $Sn_{19.3}Cu_{4.7}As_{22}I_8$, each As atom retains its tetrahedral coordination, being 1As + 3M in the case of As(2) and 4M in the case of As(1). Each metal atom is also four-coordinated, having one metal and three As neighbors. As expected, the Cu−As distances are shorter than the Sn−As distances (2.48−2.56 Å vs 2.54−2.85 Å). A fourth neighbor is different for each metal position (Figure 3): the Sn(31) atom is always connected to the Sn(31) atom at a distance of 2.82 Å, which is typical for the Sn−Sn bond in clathrates,[14−17,29] while the Sn(32) atom is always connected to the Cu(33) atom at a distance of 2.56 Å. The latter separation is quite small but is still comparable with the length of the Sn−Cu bonds found in various intermetallic compounds, where the Sn−Cu distance range is 2.52−2.90 Å.[30] Consequently, the Cu(33) atom is always bonded to the Sn(32) atom. Independent refinement of the occupancies for these positions gives practically equal values (20 ± 1% for both sites), confirming the described bonding picture. Thus, the splitting of the unique 24k position into three postions has a reasonable explanation, that is, the requirement of different bond lengths for the different metal−metal bonds.

A similar bonding picture was recently reported for the clathrates with a general formula $Sn_{17}Zn_7P_{22}X_8$ (X = I, Br).[31] For the Zn-containing clathrates, we have observed the fine splitting of the 24k metal site into three sites with partial occupancy. As in the case of $Sn_{19.3}Cu_{4.7}As_{22}I_8$, in the crystal structure of $Sn_{17}Zn_7P_{22}X_8$ one tin atom, Sn(31), is bonded to another Sn(31) atom, while the tin atom Sn(32) is bonded to the Zn(33) atom. This demonstrates the flexibility of the

(29) (a) Zhao, J.-T.; Corbett, J. D. *Inorg. Chem.* **1994**, *33*, 5721−5726. (b) Kröner, R.; Peters, K.; von Schnering, H. G.; Nesper, R. *Z. Kristallogr.−New Cryst. Struct.* **1998**, *213*, 664−665. (c) Kröner, R.; Peters, K.; von Schnering, H. G.; Nesper, R. *Z. Kristallogr.−New Cryst. Struct.* **1998**, *213*, 667−668. (d) Kröner, R.; Peters, K.; von Schnering, H. G.; Nesper, R. *Z. Kristallogr.−New Cryst. Struct.* **1998**, *213*, 669−670. (e) Kröner, R.; Peters, K.; von Schnering, H. G.; Nesper, R. *Z. Kristallogr.−New Cryst. Struct.* **1998**, *213*, 671−672. (f) Kröner, R.; Peters, K.; von Schnering, H. G.; Nesper, R. *Z. Kristallogr.−New Cryst. Struct.* **1998**, *213*, 675−676. (g) Kröner, R.; Peters, K.; von Schnering, H. G.; Nesper, R. *Z. Kristallogr.−New Cryst. Struct.* **1998**, *213*, 677−678. (h) Nolas, G. S.; Weakley, T. J. R.; Cohn, J. L. *Chem. Mater.* **1999**, *11*, 2470−2473. (i) von Schnering, H. G.; Kröner, R.; Baitinger, M.; Peters, K.; Nesper, R.; Grin, Yu. *Z. Kristallogr.−New Cryst. Struct.* **2000**, *215*, 205−206.

(30) (a) Schuster, H. U. *Naturwissenschaften* **1966**, *53*, 360−361. (b) Schuster, H. U.; Thiedemann, D.; Schoenemann, H. *Z. Anorg. Allg. Chem.* **1969**, *370*, 160−169. (c) Gangulee, A.; Das, G. C.; Bever, M. B. *Metall. Trans.* **1973**, *4*, 2063−2066. (d) Brandon, J. K.; Pearson, W. B.; Tozer, D. J. N. *Acta Crystallogr. B* **1975**, *31*, 774−779. (e) Arnberg, L.; Jonsson, A.; Westman, S. *Acta Chem. Scand. A* **1976**, *30*, 187−192. (f) Booth, M.; Brandon, J. K.; Brizard, R. Y.; Chieh, C.; Pearson, W. B. *Acta Crystallogr. B* **1977**, *33*, 30−36. (g) Barkov, A. Y.; Laajoki, K. V. O.; Gornostayev, S. S.; Pachomovskii, Ya. A.; Men'shikov, Yu. P. *Am. Mineral.* **1998**, *83*, 901−906.

(31) Kovnir, K. A.; Shatruk, M. M.; Reshetova, L. N.; Presniakov, I. A.; Dikarev, E. V.; Baitinger, M.; Haarmann, F.; Schnelle, W.; Baenitz, M.; Grin, Yu.; Shevelkov, A. V. *Solid State Sci.* **2005**, *7*, 957−968.

Table 3. Selected Interatomic Distances and Bond Angles in the Structure of $Sn_{19.3}Cu_{4.7}As_{22}I_8$[a]

		Distance within the Framework, Å	
Sn(31)−As(1)	2.536(2)	Cu(33)−As(1)	2.56(1)
Sn(31)−As(2)	2.594(3) × 2	Cu(33)−As(2)	2.484(8) × 2
Sn(31)−Sn(31)	2.82(1)	Cu(33)−Sn(32)	2.56(1)
Sn(32)−As(1)	2.678(5)	As(2)−As(2)	2.413(2)
Sn(32)−As(2)	2.847(7) × 2	*Sn(31)−Sn(32)*	*0.22(2)*
Sn(32)−Cu(33)	2.56(1)	*Sn(31)−Cu(33)*	*0.50(2)*
		Sn(32)−Cu(33)	*0.71(2)*
		Host−Guest Distances, Å	
I(1)−As(2)	3.631(2)	I(2)−Sn(32)	3.532(5)
I(1)−Cu(33)	3.689(2)	I(2)−Sn(31)	3.782(4)
I(1)−Sn(31)	3.737(2)	I(2)−Cu(33)	3.927(5)
I(1)−Sn(32)	3.765(3)	I(2)−As(1)	3.950(5)
		I(2)−As(2)	4.130(5)
		Angles, deg	
As(1)−Sn(31)−As(2) × 2	107.2(1)	As(1)−Sn(32)−Cu(33)	140.6(4)
As(2)−Sn(31)−As(2)	107.8(2)	As(2)−Sn(32)−Cu(33) × 2	109.5(2)
As(1)−Sn(31)−Sn(31)	123.1(1)	As(1)−Cu(33)−As(2) × 2	110.0(3)
As(2)−Sn(31)−Sn(31) × 2	105.4(1)	As(2)−Cu(33)−As(2)	115.1(6)
As(1)−Sn(32)−As(2) × 2	96.7(3)	As(1)−Cu(33)−Sn(32)	111.0(6)
As(2)−Sn(32)−As(2)	94.9(3)	As(2)−Cu(33)−Sn(32) × 2	105.3(3)

[a] The short metal−metal contacts (italicized) correspond to the fine splitting of the 24k position.

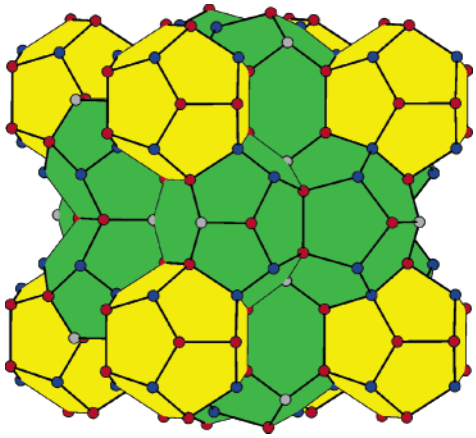

Figure 1. Polyhedral presentation of the clathrate-I structure: 24k position, red circles; 16i position, blue circles; 6i position, gray circles; pentagonal dodecahedra, yellow; tetrakaidecahedra, green.

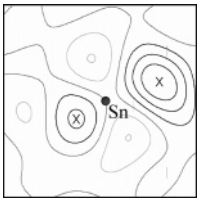

Figure 2. Difference Fourier density map near the 24k metal position in the crystal structure of $Sn_{19.3}Cu_{4.7}As_{22}I_8$ for the model with only one fully occupied Sn atom in the position of Sn(31). Crosses mark the position of Cu(33), left, and Sn(32), right, further introduced into refinement. Black and gray contours represent positive and negative electron density, respectively.

tin−pnictogen framework. Independently of the amount and the nature of the d metal, the required atomic distribution for the optimal framework bonding is achieved.

The splitting of the 24k position into three positions in the crystal structure of $Sn_{19.3}Cu_{4.7}As_{22}I_8$ has important consequences. The Sn(32) atom adopts a very distorted tetrahedral coordination of three rather distant As atoms and one closely lying Cu atom (cf. Table 3). Compared to the Sn(31) and Cu(33) atoms, the Sn(32) atom is relatively

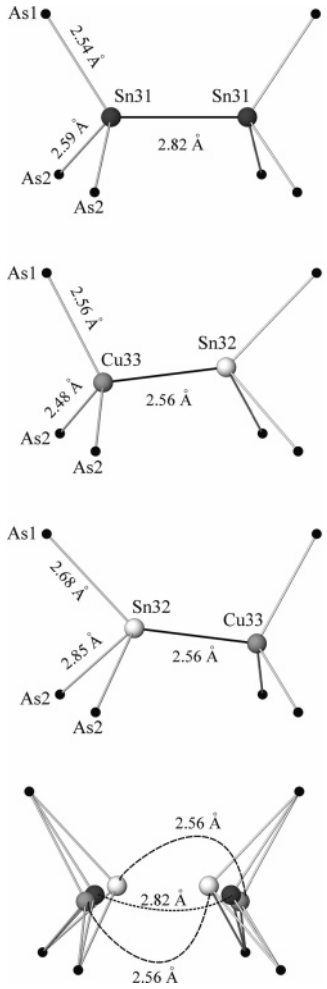

Figure 3. Local atomic connections around the 24k 3-fold split metal atom position M3 in the crystal structure of $Sn_{19.3}Cu_{4.7}As_{22}I_8$ (for an explanation, see the text).

loosely bound and, consequently, has a larger atomic displacement parameter. Moreover, the position of the Sn(32) atom is shifted from the ideal 24k position of the clathrate-I structure toward the I(2) atom. Taking into account

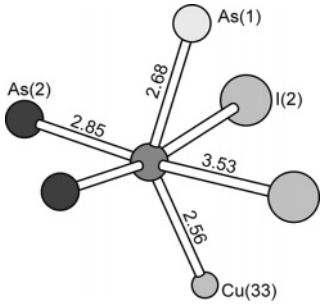

Figure 4. Environment of the Sn(32) atom. Interatomic distances are given in angstroms.

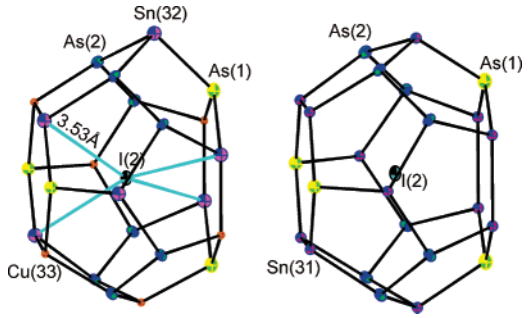

Figure 5. Tetrakaidodecahedron around the I(2) atom in the crystal structure of $Sn_{19.3}Cu_{4.7}As_{22}I_8$. Two ordered variants are shown: Sn(32) and Cu(33) at 24k, left; Sn(31) at 24k, right (for an explanation, see the text). Light-blue lines indicate the shortest Sn(32)−I(2) contacts. All atoms are drawn as thermal ellipsoids at 50% probability.

two I atoms as second-sphere neighbors, the coordination polyhedron of the Sn(32) atom can be extended to an extremely distorted octahedron (Figure 4). The separation between the Sn(32) and I(2) atoms is only 3.53 Å, which is at least 0.25 Å shorter than other separations between the I(2) atom and the atoms of the framework. Taking into account that the Sn(31)−Sn(31) and Sn(32)−Cu(33) pairs alternate, the extreme statistically probable polyhedron around the I(2) atom can contain either only Sn(31) or Sn(32) and Cu(33) atoms at the 24k position (Figure 5). In the latter case, the I(2) atom has four rather short Sn(32) neighbors located at the opposite hexagonal faces of the tetrakaidecahedron, explaining the large and anisotropic displacement parameter for the I(2) atom.

To confirm the fine splitting of the metal site in the structure of $Sn_{19.3}Cu_{4.7}As_{22}I_8$, we recorded the ^{119}Sn Mössbauer spectrum shown in Figure 6. The spectrum is best fitted as a superposition of two quadrupole doublets (the parameters are listed in Table 4). The intensities of the doublets, 72(2) and 28(2)%, correspond, within the experimental errors, to the crystallographic occupancies of the respective Sn sites in the crystal structure of $Sn_{19.3}Cu_{4.7}As_{22}I_8$ [75% of tin in the Sn(31) position and 25% in the Sn(32) position]. Table 4 shows that the isomer shift (δ = 2.12 mm s^{-1}) and quadrupole splitting (Δ = 0.61 mm s^{-1}) for Sn(31) are close to the values reported for $Sn_{24}P_{19.3(2)}\square_{2.7(2)}I_8$[16] and for $Sn_{17}Zn_7P_{22}X_8$ (X = I, Br),[31] indicating the four-coordinated tin atom bonded to three pnictogen atoms and one tin atom. A small increase of the isomer chemical shift arises from the less electronegative pnictogen (As) bonded to the

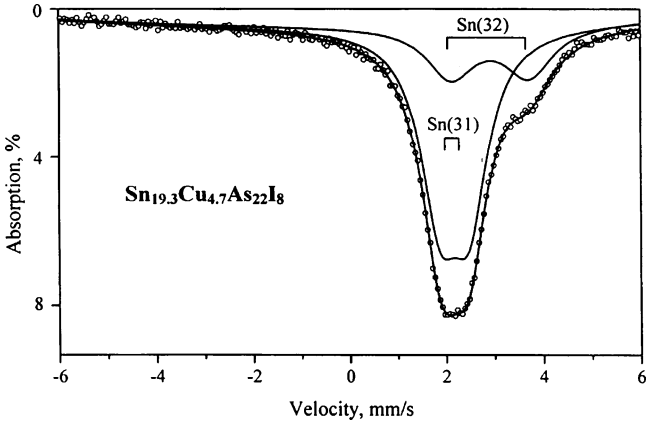

Figure 6. ^{119}Sn Mössbauer spectrum for $Sn_{19.3}Cu_{4.7}As_{22}I_8$. Solid lines show the fitting doublets. In the top of the spectrum, square brackets show the location of the doublets.

Sn atom, while the smaller quadrupole splitting merely reflects the smaller distortion of the Sn tetrahedral environment.

The analysis of the data compiled in Table 4 shows that the isomer shift for the second component, Sn(32), of $Sn_{19.3}Cu_{4.7}As_{22}I_8$ (δ = 2.88 mm s^{-1}) is significantly larger than those found for all other cationic clathrates including the isostructural $Sn_{17}Zn_7P_{22}X_8$ (X = Br, I) phases.[31] Moreover, it is accompanied by a larger, compared to those of $Sn_{17}Zn_7P_{22}X_8$, value of the quadrupole splitting (Δ = 1.62 mm s^{-1}), which is quite unexpected because for the covalent Sn compounds the increase in the isomer shift value typically leads to the diminution of the quadrupole splitting.[32] Indeed, the increase of the isomer shift normally reflects the increase of the s character near the Sn atomic nuclear, rendering symmetric distribution of the electron density around the ^{119}Sn and, thus, leading to lower values of the quadrupole splitting.

To determine the factors governing the values of the δ and Δ parameters, we performed calculations according to the Townes−Dailey model,[33] which proved to be a useful tool for interpreting the ^{119}Sn Mössbauer spectra of tin clathrates.[16] In the frames of this semiempirical model, the observed value of Δ is represented as

$$\Delta = \Delta_o\{2\alpha^2 C_p^{\,2} + \sum_{i=1}^{3}\alpha_i^{\,2}[2C_{z(i)}^{\,2} - (C_{x(i)}^{\,2} + C_{y(i)}^{\,2})]\} \quad (1)$$

where Δ_o = 3 mm s^{-1} is a quadrupole splitting produced by a single electron occupying a p_z orbital.[33] The coefficients α^2 and α_i^2 describe the contribution of a given hybrid tin orbital to the molecular orbital localized along the respective bond:

$$\Psi_{Sn-M} = \alpha h_{Sn-M} + (1-\alpha^2)^{1/2}\phi_M \quad (2a)$$

$$\Psi^{(i)}_{Sn-X} = \alpha_i h^{(i)}_{Sn-X} + (1-\alpha^2)^{1/2}\phi^{(i)}_X \quad (2b)$$

where ϕ_M and ϕ_X are the atomic (hybrid) orbitals of M (=Sn,

(32) Flinn, P. A. In *Mossbauer Isomer Shifts*; Shenoy, G. K., Wagner. F. E., Eds.; North-Holland: Amsterdam, The Netherlands, 1978; p 593.
(33) Townes, C. H.; Dailey, B. P. *J. Chem. Phys.* **1949**, *17*, 782−799.

Table 4. Fitting Parameters of the ^{119}Sn Mössbauer Spectrum for the Clathrates with the Cationic Framework

compound	Sn coordination	δ in mm s^{-1}, ±0.01	Δ in mm s^{-1}, ±0.01	I in %, ±2	ref
$Sn_{24}P_{19.3(2)}\square_{2.7(2)}I_8$	1Sn + 3P	1.84	0.72	73	14, 16
	1Sn + 2P + 3Sn[a]	2.55	0.44	27	
$Sn_{14}In_{10}P_{21.20.8}I_8$	1M + 3P[b]	1.83	1.35	88	16
	1M + 2P + 3M[a,b]	2.56	0.30	12	
$Sn_{10}In_{14}P_{22}I_8$	1M + 3P[b]	1.77	1.34	100	16
$Sn_{17}Zn_7P_{22}I_8$	1Sn + 3P	2.04	0.79	53	31
	1Zn + 3P	2.66	1.53	47	
$Sn_{17}Zn_7P_{22}Br_8$	1Sn + 3P	1.99	0.97	47	31
	1Zn + 3P	2.66	1.57	53	
$Sn_{19.3}Cu_{4.7}As_{22}I_8$	1Sn + 3As	2.12	0.61	72	this work
	1Cu + 3As	2.86	1.62	28	

[a] Distorted octahedral coordination, best described as the 3 + 3 environment. [b] M is statistically Sn or In.

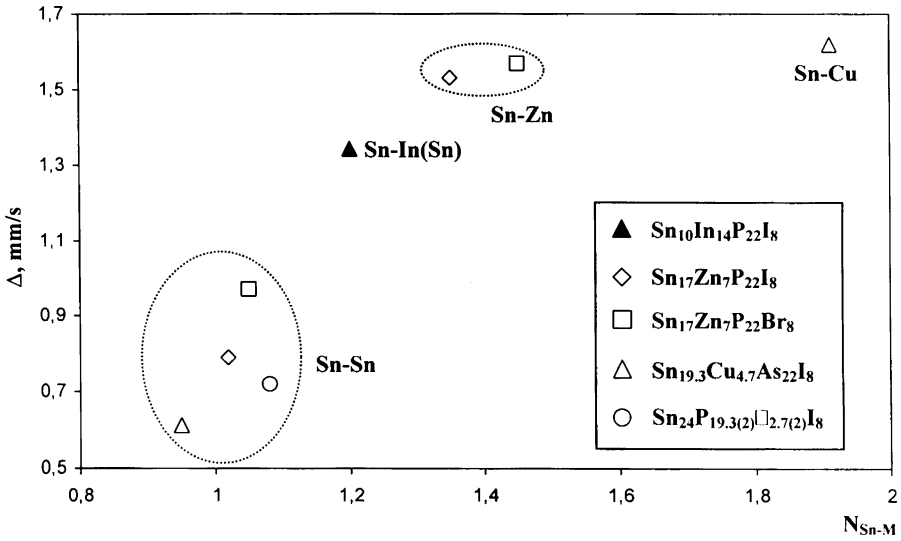

Figure 7. Quadrupole splitting in the ^{119}Sn Mossbauer spectra for different coordination of Sn atoms in the cationic clathrates as a function of the population of the hybrid Sn orbital participating in the Sn−M bonding.

Zn, In, Cu) and X (=P, As), respectively, and h_{Sn-M} and h_{Sn-X} are the hybrid orbitals of Sn responsible for the formation of the Sn−M and Sn−X bonds, respectively:

$$h_{Sn-M} = C_s s + C_p p_z \quad (3a)$$

$$h^{(i)}_{Sn-X} = C_{s(i)} s + C_{z(i)} p_z + C_{x(i)} p_x + C_{y(i)} p_y \quad (3b)$$

where C_s, C_p, and $C_{s,z,x,y(i)}$ are the coefficients for the Sn atomic orbitals forming a respective hybrid orbital. These coefficients are defined only by the geometry of a coordination polyhedron around a given Sn atom. Using the geometry of the Sn atom environment shown in Table 3 for $Sn_{19.3}Cu_{4.7}As_{22}I_8$ and those published previously for some other tin cationic clathrates,[14,16,31] we calculated the C_s, C_p, and $C_{s,z,x,y(i)}$ coefficients for the (3a) and (3b) hybrids as described in detail in the literature.[34] Then, we calculated the α_i coefficients for the molecular orbitals (2b) from the Pauling electronegativity coefficients χ, Sn(1.96), As(2.18), and P(2.19) as $\alpha^2 = [1 - (1/2)\Delta\chi]/2$. Substitution of all of these data into (1) enabled us to calculate the population ($2\alpha^2$ because two electrons can occupy a single orbital) of the hybrid orbitals (2a) for the observed values of Δ shown in Table 4.

The results of the calculations are plotted in Figure 7 for different Sn−M bonds. It is obvious that the population of the Sn hybrid orbital in the case of the Sn−Sn bond is around unity, being in accordance with the covalent character of the homonuclear Sn−Sn bond. On the contrary, all other Sn hybrid populations, $2\alpha^2$, are higher than unity and depend on the nature of the metal forming the Sn−M bond. For instance, the corresponding values for the Sn hybrid orbital participating in the Sn−Zn bond are 1.35 and 1.45 for X = I and Br, respectively, with the higher value indicating the shorter Sn−Zn distance and the consequent higher population of the Sn hybrid orbital. The hybrid orbital population for the Sn atom bonded to the Cu atom in $Sn_{19.3}Cu_{4.7}As_{22}I_8$ is much higher; it reaches the value of 1.91. Assuming that Sn−Cu is a two-electron, two-center (2e−2c) bond, this value means that the bonding electron pair occupies the orbital that is predominantly Sn in nature. In general, the analysis of the data shown in Figure 7 suggests that the population of the (3a) hybrid depends not on the Pauling electronegativity of the M atom but rather on its formal charge. According to the Zintl scheme applicable to the electron count in cationic clathrates,[9] the Cu atom ($4s^1$) requires three electrons to form four 2e−2c bonds, which is one electron more than is needed by Zn and two electrons more than is required by In, while Sn does not need extra

(34) Nikitin, O. Yu.; Novosadov, B. K. *J. Struct. Chem.* **1995**, *36*, 969−976.

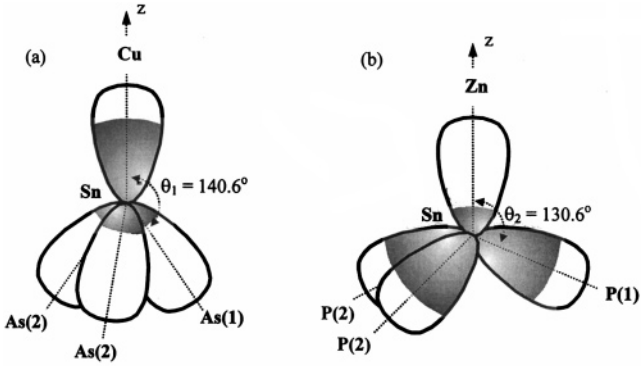

Figure 8. Calculated contribution of the s orbitals (shaded area) to the Sn hybrid orbitals as a function of the θ angle for the Sn atom bonded to the Cu atom in $Sn_{19.3}Cu_{4.7}As_{22}I_8$ (a) and for the Sn atom bonded to the Zn atom in $Sn_{17}Zn_7P_{22}I_8$ and $Sn_{17}Zn_7P_{22}Br_8$ (b).

electrons. Accordingly, the population of the (3a) hybrid forming the Sn−Sn bond is unity, and it increases on going through In and Zn to Cu.

The calculations also showed that the contribution of the Sn s and p_z orbitals to the (3a) hybrid responsible for the Sn−M bonding is different in $Sn_{19.3}Cu_{4.7}As_{22}I_8$ and $Sn_{17}Zn_7P_{22}X_8$, which is schematically depicted in Figure 8. It is clear from the drawings that the higher the θ angle, the higher the s-orbital contribution to the (3a) hybrid. In turn, a higher s-orbital contribution to the Sn−Cu bond in $Sn_{19.3}Cu_{4.7}As_{22}I_8$ leads to a higher isomer shift, as soon as the withdrawal of the electron density by the electronegative atoms, $\chi(P) = 2.19$ and $\chi(As) = 2.18$, is similar in the two cases. Accordingly, the p_z contribution to the hybrid orbital (3a) is smaller in $Sn_{19.3}Cu_{4.7}As_{22}I_8$, which would imply a smaller electrical field gradient and a correspondingly smaller quadrupole splitting. However, the very high population ($2\alpha^2 = 1.91$) of the Sn hybrid orbital (3a) in $Sn_{19.3}Cu_{4.7}As_{22}I_8$ causes the alternative effect, that is, an increase of the electric field gradient produced by the great asymmetry of the electron density around the Sn atom. Therefore, the quadrupole splitting is also higher for the Sn(32) component in $Sn_{19.3}Cu_{4.7}As_{22}I_8$.

In the vacancy-free compounds $Sn_{19.3}Cu_{4.7}As_{22}I_8$ and $Sn_{17}Zn_7P_{22}X_8$ (X = Br, I),[31] the fine splitting of the 24k metal position arises from the different requirements for the metal−metal bonding. Such a splitting leads to two different types of tetrahedrally coordinated Sn atoms: Sn(31) having a 3As + 1Sn(31) environment and Sn(32) having 3As + 1M (M = Cu or Zn) coordination. In the vacancy-containing compounds $Sn_{24}P_{19.3(2)}\square_{2.7(2)}X_8$ (X = I, Br), the fine splitting of the 24k metal position was also found,[14,17] but in that case, it is the presence of the vacancies at the phosphorus site that causes the splitting. The tin atom Sn(31) has the 3P + 1Sn tetrahedral coordination as in the case of the vacancy-free compounds. However, the tin Sn(32) atom, which is associated with the vacancy, has a distorted octahedral coordination, which is best described as a 3 + 3 environment, where three shorter distances refer to two Sn−P bonds of 2.7 Å and one Sn−Sn bond at 2.9 Å while three longer distances are the Sn−Sn contacts ranging from 3.15 to 3.3 Å. Such a difference in Sn coordination clearly manifests itself in the Mössbauer spectra: the (3 + 3)-coordinated Sn atom causes only a small quadrupole splitting of 0.30−0.44 mm s^{-1} in $Sn_{24}P_{19.3}I_8$ and $Sn_{14}In_{10}P_{21.2}I_8$ (see Table 4), indicating high suppression of the stereoactivity of the lone pair on a Sn atom.

Recently, different variants of the superstructure of the clathrate-I type were found for the vacancy-containing clathrates.[16,35,36] These complicated superstructures arise because of a partial or full ordering of vacancies in the framework. It seems reasonable to expect in $Sn_{19.3}Cu_{4.7}As_{22}I_8$ a superstructure resulting from the ordering of the metal sites. However, superstructure reflections were observed neither in single-crystal diffraction nor in powder X-ray diffraction patterns of $Sn_{19.3}Cu_{4.7}As_{22}I_8$. Investigation by ED, sensitive to weak and local ordering phenomena, also did not reveal any superstructure ordering. In Figure 9, the ED patterns for $Sn_{19.3}Cu_{4.7}As_{22}I_8$ along the main zones are shown. These ED patterns can be completely indexed in the cubic $Pm\bar{3}n$ space group using the unit cell parameters determined by X-ray diffraction (see Table 1). No superstructure spots or diffuse intensities are present in the diffraction patterns. Also, the [001] HREM image is perfectly in agreement with the expected (simulated) image based on the crystal structure data given in Table 1 (Figure 10). No planar defects or imperfections have been observed. Apparently, the fine splitting of the 24k position into three positions with partial occupancies does not result in the appearance of an ordered superstructure. The presence of vacancies in the clathrate framework might be a necessary condition for the superstructure formation; this study is currently underway.

The composition of the tin−copper arsenide iodide was predicted using the Zintl formalism. Earlier we showed that this concept is applicable for prognostication of the composition of clathrates with a cationic framework. In the case of the tin,[14,17] tin−indium,[16] and tin−zinc[31] phosphide iodides, we observed a good agreement between the predicted and experimentally determined compositions. According to the Zintl formalism, each atom realizes its electron octet. For clathrates with cationic frameworks, this means that four electrons per framework atom and one electron for each halogen atom are necessary. In the case of the title compound, each Sn atom has the required amount of four electrons, each As atom has one extra electron, each Cu atom needs three additional electrons, and each I guest atom needs one electron. For the charge-balanced compound $Sn_{24-x}Cu_xAs_{22}I_8$, x must be equal to $(22 - 8)/3 \approx 4.67$, which is essentially the same as that in $Sn_{19.3}Cu_{4.7}As_{22}I_8$. Cu is a transition metal, while Zn is not; however, the same electron-counting scheme is applicable for the Zn- and Cu-containing clathrates, with the only difference being the number of valence electrons. Compared to Cu, Zn has one electron more; therefore, it requires two electrons to complete the octet; then, for the charge-balanced, vacancy-free clathrate $Sn_{24-x}Zn_xPn_{22}X_8$ (Pn = P or As; X = Br or I), x must be equal to $(22 - 8)/2 = 7$.[31] In this work, the investigation of

(35) Carrillo-Cabrera, W.; Budnyk, S.; Prots, Yu.; Grin, Yu. *Z. Anorg. Allg. Chem.* **2004**, *630*, 2267−2276.
(36) Dubois, F.; Fässler, T. F. *J. Am. Chem. Soc.* **2005**, *127*, 3264−3265.

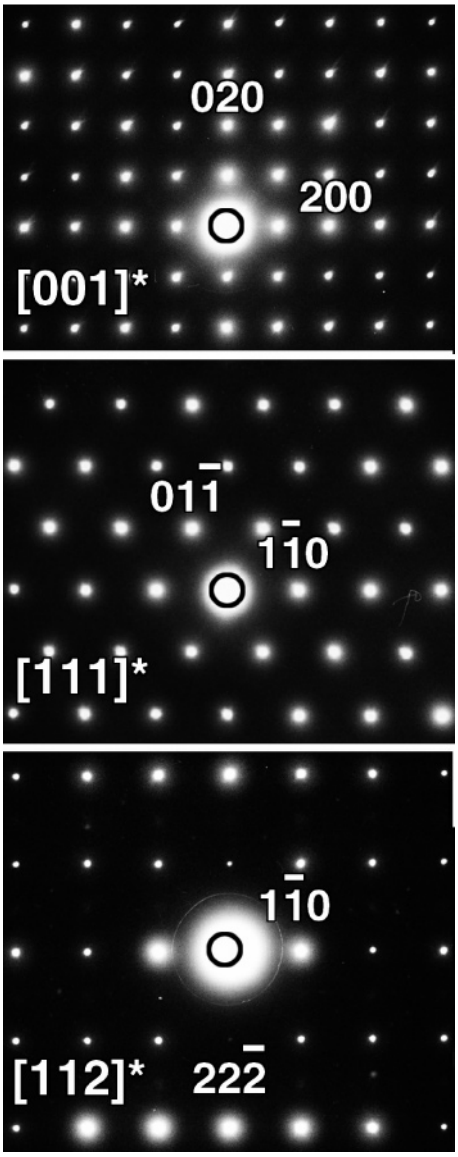

Figure 9. ED patterns along the major zones [001]*, [111]*, and [112]* of $Sn_{19.3}Cu_{4.7}As_{22}I_8$.

the temperature dependence of the magnetic susceptibility $\chi(T)$ for $Sn_{19.3}Cu_{4.7}As_{22}I_8$ revealed the diamagnetic behavior expected for the Zintl phase. The same behavior was earlier observed for the Zn-containing clathrates with the cationic framework.[31]

In conclusion, $Sn_{19.3}Cu_{4.7}As_{22}I_8$ is a new type-I cationic clathrate, the first one to contain a transition metal in the cationic framework. Its crystal structure reveals a complicated

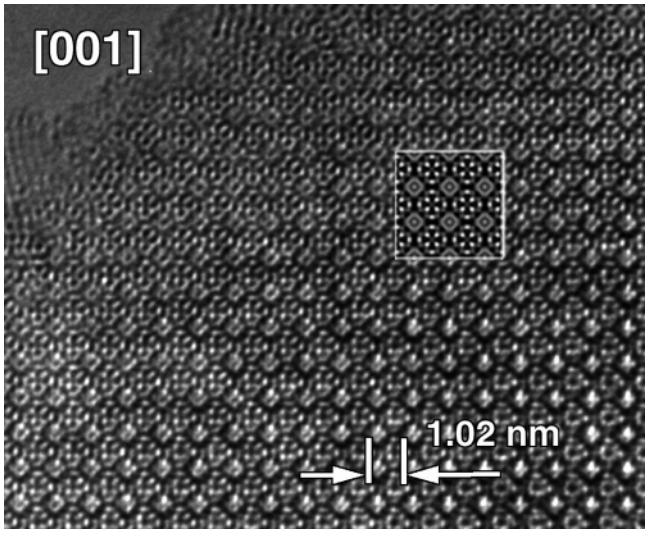

Figure 10. HREM image along the [001] zone for $Sn_{19.3}Cu_{4.7}As_{22}I_8$. The calculated image for a defocus value Δf of -30 nm and a thickness of 6 nm is given as an inset.

local ordering within the clathrate framework resulting in the splitting of the 24-fold position into three partially occupied sites, which, however, does not lead to any detectable superstructure. The splitting is caused by the different bond distance requirements of the atoms composing the framework, in particular by the difference in the Sn−Sn and Sn−Cu bond distances. The latter 2c−2e bond is polar, showing the paramount population of a Sn hybrid orbital participating in the Sn−Cu bonding orbital. $Sn_{19.3}Cu_{4.7}As_{22}I_8$ is diamagnetic, and its composition can be rationalized in terms of the Zintl concept.

Acknowledgment. The authors thank U. Köhler for help in the magnetization measurements, U. Schmidt and Dr. G. Auffermann for chemical analysis, and Dr. M. Baitinger for discussion. This research is supported by the Russian Foundation for Basic Research (Grant 03-03-32514a), the U.S. Civilian Research & Development Foundation for the Independent States of the Former Soviet Union (Award No. 12735), and the European Commission 5th Framework Program (Contract HPRN-CT-2002-00193). K.A.K. thanks the Max-Plank Society for a research fellowship.

Supporting Information Available: Information on the structural experiment (CIF). This material is available free of charge via the Internet at http://pubs.acs.org.

IC051160K